3.2.3 Flux-Weakening Control Design and Analysis

In order to produce the maximum torque, which main component is proportional to q-axis component of the armature current [58], Eq.s (12), it is convenient to control the inverter-fed PMSM by keeping the direct, *d-axis*, current component to be $i_d = 0$ as long as the inverter output voltage doesn't reach its limit [42]. At that point, the motor reaches its maximum speed, so-called *rated speed* (called also *base speed* when talking about flux-weakening). Beyond that limit, the motor torque decreases rapidly toward its minimum value, which depends on a load torque profile. To expand the speed above the rated value, the motor torque is necessary to be reduced. A common method in the control of synchronous motors is to reduce the magnetizing current, which produces the magnetizing flux. This method is known as *field-weakening* [64]. With PM synchronous motors it is not possible, but, instead, the air gap flux is weakened by producing a negative d-axis current component, i_d. Because nothing has happened to the excitation magnetic field and the air gap flux is still reduced, so is the motor torque, this control method is called *flux-weakening* [69]. As a basis for this analysis, the PMSM current and voltage d-q vector diagrams from the previous section, Figure 26, are used. During flux-weakening, because the demagnetizing (negative) i_d current increases, a phase current vector i_s rotates toward the *negative d-semiaxis*. The rotation of the phase voltage vector is determined by a chosen flux-weakening strategy, but at the end of flux-weakening it always rotates toward the *positive q-semiaxis* because of i_q current, i.e. v_d voltage magnitude decrease. Hence, the voltage-to-current phase shift decreases to zero and increases in negative direction either to the inverter phase shift limit (usually 30^0) [65], or a load torque dictated steady-state (zero acceleration), or to the zero motor torque condition (no load or generative load). A big concern of flux-weakening control is a danger of permanent demagnetization of magnets. However, large coercitivity of materials such as Samarium-Cobalt, allows significant i_d current which can extend the motor rated speed up to two times [58, 61-63, 70]. Three commonly used flux-weakening control strategies are:

1) constant-voltage-constant-power (CVCP) control;
2) constant-current-constant-power (CCCP) control; and
3) optimum-current-vector (OCV or CCCV - constant-current-constant-voltage) control.

3.2.3.1 Constant Voltage Constant Power (CVCP) Control

This strategy is very popular in industry because of its simplicity [63, 69]. It is based on keeping the voltage steady-state d and q components constant:

$$\begin{aligned}
&P_m = T_m w = \frac{3}{2}\left(v_d i_d + v_q i_q\right) = const. \\
&v_d \approx -pL_q w\, i_q = -pL_q W_b I_{qb} = const. \\
&v_q \approx k_t w + pL_d w\, i_d = k_t W_b = const. \\
&v_s = V_{s\,max} = V_{qb} = const.
\end{aligned} \tag{73}$$

Values v_{qb}, i_{qb} and W_b are base voltage, base current and base (rated) speed in the beginning of the flux-weakening, respectively. Usually, $I_{qb} = I_{s\max}$.

Reference i_d and i_q currents are derived from (73):

$$\begin{aligned}
&i_d = -\frac{k_t}{pL_d}\left(1 - \frac{W_b}{w}\right) \\
&i_q = I_{qb}\frac{W_b}{w}
\end{aligned} \tag{74}$$

Regarding the complexity, this is the easiest flux-weakening control, due to i_d / i_q linearity, which is obvious from (74).

By this strategy, the voltage vector V_s on the PMSM voltage vector diagram, Figure 26.b, is supposed to keep a constant position, while the vertex of the current vector, i_s, moves from point (0, I_{qb}) down the slope i_q / i_d, derived from Eq. (74) toward the *negative d-semiaxis*. The current and voltage d-q vector tendencies in CVCP flux-weakening control strategy are shown in Figure 28. However, when the phase current limit, Figure 24, is reached, i.e. after passing the critical speed, ω_{cr}, the strategy fails and vector I_s follows the limitation circle, while vector V_s naturally rotates toward the v_q-axis. The critical speed, where the current reaches its limit is:

$$w_{cr} = \frac{I_p^2 + I_{qb}^2}{I_p^2 - I_{qb}^2} W_b = \frac{V_{qb}^2 + V_d^{'2}}{V_{qb}^2 + V_d^{'2}} W_b \tag{75}$$

where

$$I_p = \frac{k_t}{pL_d} \quad \text{and} \quad V_d^{'} = \frac{L_d}{L_q} V_d \tag{76}$$

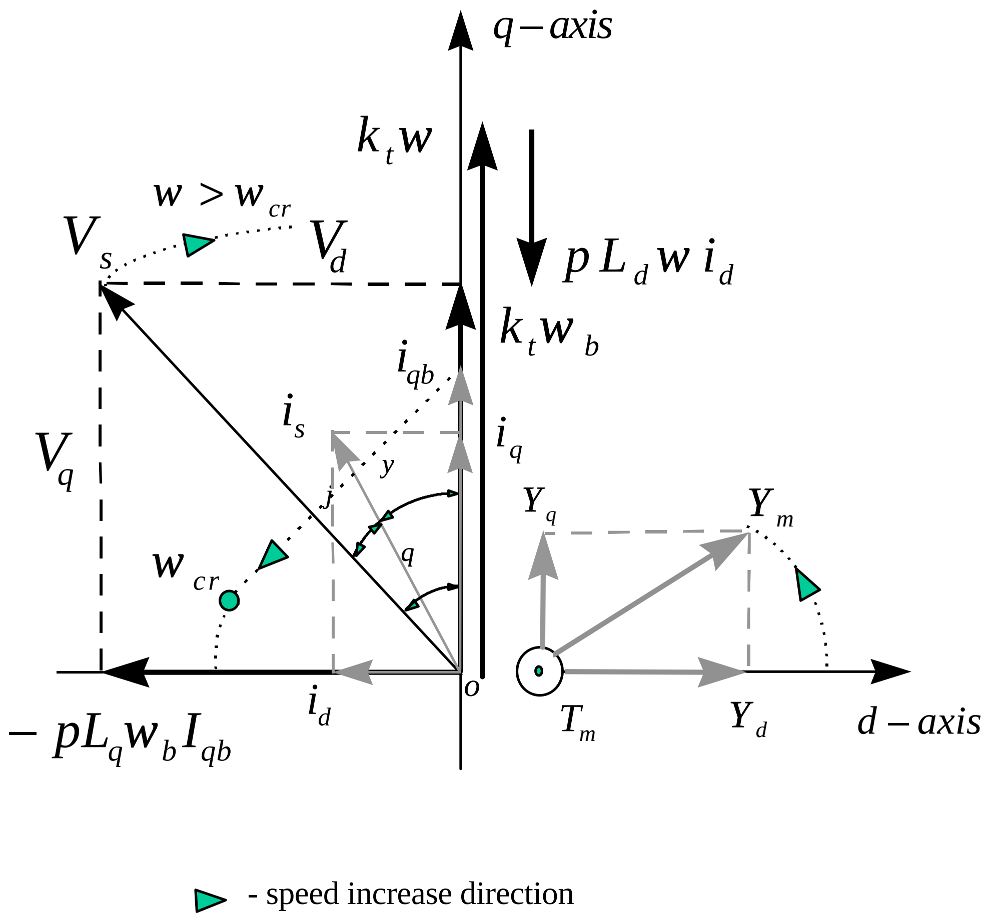

Figure 28. PMSM voltage d-q vector diagram for CVCP flux-weakening control

The derivation of Eq. (75) is given in Appendix B.

If we want to be precise, the phase voltage vector v_s doesn't stay constant at $\omega \leq \omega_{cr}$. Vector v_s rotates toward the *negative d-semiaxis*, in the same direction as the current vector, but much slower. This rotation of v_s occurs because of transients $di_d / dt < 0$ and $di_q / dt < 0$ in Eq.s (12). Another, usually neglected, fact is that the active power is not constant either, which can be seen in the simulation results in Chapter 4. In order to get constant power, the following condition must be satisfied:

$$Ri_d^2 + Ri_q^2 - RI_{qb}^2 \approx p\left(L_q - L_d\right)w\, i_q i_d \tag{77}$$

It should also be noticed from Eq. (76) that for one quadrant motor operation, ω_{cr} will never be reached if $I_p \leq I_{qb}$, which means $v_{qb} \leq v_{db}$, which implies voltage-to-current phase shift $j \geq 45^o$. Since that means a poor motor efficiency before the flux-weakening region (small motor torque versus current ratio), this option, in this application, is of only theoretical character. If a goal is a speed higher than w_{cr}, with this control strategy, motor torque T_m would decrease more rapidly after crossing w_{cr}, following the current-vector-limit circle, instead of the reference current ramp of the CVCP control, up to an earlier defined maximum speed. The optimum case is that ω_{cr} is designed to be close to a desired maximum motor speed.

Finally, the power factor, cosφ, can be calculated from:

$$\begin{aligned} &\cos j = \cos(q - y) \\ &y = \tan^{-1}\left(\frac{-i_d}{i_q}\right), \quad q = \tan^{-1}\left(\frac{-v_d}{v_q}\right) \end{aligned} \tag{78}$$

where j, q and y are vector phase shifts from Figure 26. Eq. (78) can be used for determination of the speed when $\cos j$ reaches its minimum tolerable value, determined by the inverter limitation.

3.2.2.2 Constant Current Constant Power (CCCP) Control

A characteristic of this method is that neither i_q, nor i_d current depends on the motor parameters. The i_q current has the same expression as in the previous strategy, due to keeping the power constant [66]. That implies that v_d voltage is also constant, Figure 29. However, the phase voltage *q-axis* component, v_q, depends on both, motor parameters and the current *q-axis* component base value, Eq.s (12) and (79).

The references for this control method are:

$$\begin{aligned} i_s &= I_{qb} = const. \\ P_m &= T_m w = \frac{3}{2}\left(v_d i_d + v_q i_q\right) = const. \end{aligned} \tag{79}$$

From Eq.s (12) and (79), reference i_d and i_q currents for the current control loops are:

$$\begin{aligned} i_q &= I_{qb}\frac{W_b}{w} \\ i_d &= -\sqrt{I_{qb}^2 - i_q^2} \end{aligned} \tag{80}$$

The d-q voltage equations in steady-state, extracted from Eq.s (12) and (79) are:

$$\begin{aligned} v_d &= -pL_q w i_q = const. \\ v_q &= -pL_d w i_d + k_t w \end{aligned} \tag{81}$$

By applying this strategy, the phase current vector i_s rotates around its origin, and phase voltage vector v_s, vertex moves along the $v_d = -pL_q w_b I_{qb}$ line, Figure 29. The prevailing speed, ω_p, where voltage v_q passes its minimum is

$$w_p = \frac{W_b}{\sqrt{1-\left(-\frac{V_d^{'}}{V_{qb}}\right)^2}} \Rightarrow v_q = v_{q\,min} \tag{82}$$

where $V_d^{'} = \frac{L_d}{L_q}V_d$ and $V_{qb} = k_t W_b$.

A critical speed when voltage v_s reaches its maximum value is the same as in the previous example, but now the phase current i_s reaches its limit:

$$w_{cr} = \frac{I_p^2 + I_{qb}^2}{I_p^2 - I_{qb}^2} W_b = \frac{V_{qb} + V_d^{'}}{V_{qb} + V_d^{'}} W_b \tag{83}$$

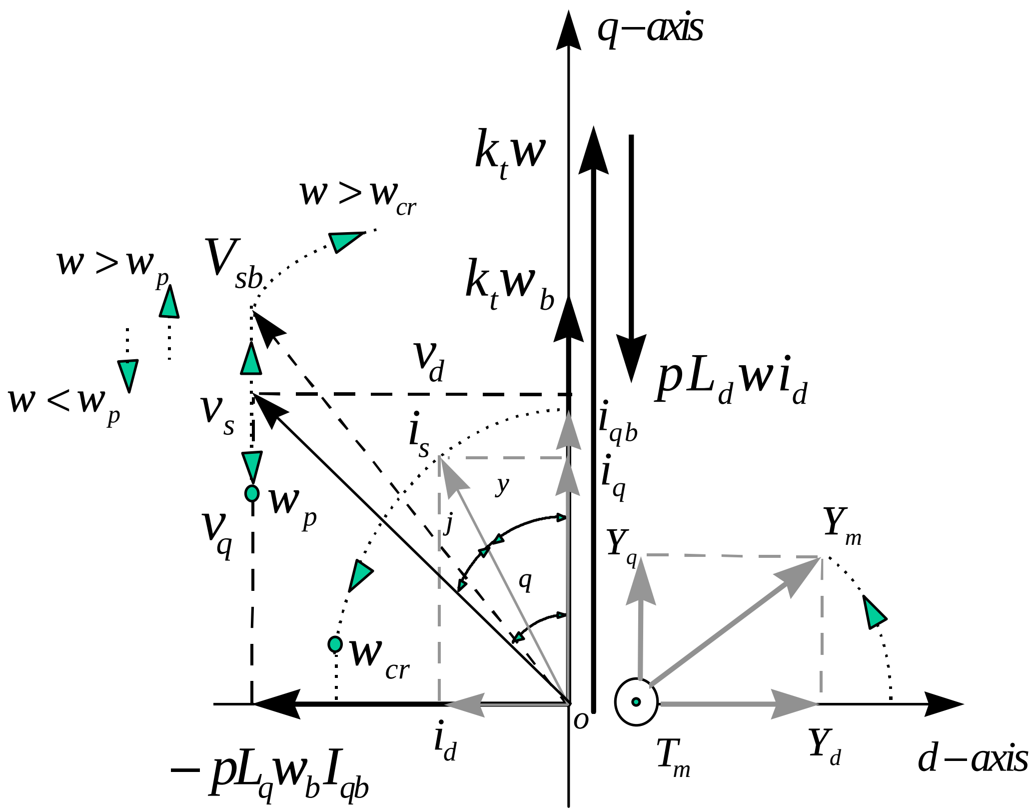

- speed increase direction

Figure 29. PMSM voltage d-q vector diagram for CCCP flux-weakening control

When $\omega = \omega_{cr}$, the phase voltage reaches its limit and stays constant under higher speed. It causes a rapid decrease of current i_q , what implies the decrease of the motor torque, T_m, Eq.s (12). Detailed mathematical derivations are given in Appendix B.

Because transient elements di_q/dt and di_d/dt from the d-q voltage equations from Eq.s (12) cancel each other in Eq. (79), active power P_m remains constant during the flux-weakening period until the critical speed is reached. It is characteristic for both constant power control methods that the *d-axis* steady-state voltage component remains constant as long as both voltage and current don't reach their limits. In comparison with the constant voltage strategy, this strategy is more complex because of the reference i_d/i_q non-linearity. Its advantages are constant phase current and constant power in flux-weakening region between W_b and w_{cr}. Different torque slopes, obtained after $\omega = \omega_{cr}$, are consequences of applied strategies, as well as of applied voltage limitation methods. The same method doesn't produce the same effect on both strategies (see Table 2). How strong the effect is, how big the difference is, and what profiles the motor torque obtains after $\omega = \omega_{cr}$, also depends on motor characteristics and current and speed base values, as well as the load torque profile (Table 2). This investigation remains for future work.

3.2.3.3 Optimum Current Vector (OCV) Control

Unlike the constant power flux-weakening control strategies, where phase voltage or current were reduced in order to keep constant active power, in this method the active power is allowed to change with a change of the power factor, $\cos j$, while the magnitudes of phase current and phase voltage vectors are set to their maximum values [51, 65]:

$$\begin{aligned} i_s &= I_{qb} = I_{s\,max} = const. \\ v_s &= V_{qb} = V_{s\,max} = const. \end{aligned} \tag{84}$$

In other words, by this control strategy the maximum allowable apparent power is used, although the active power is not constant. Hence, both vector trajectories are along their limiting circles, Figure 24 and Figure 25. The superimposed current, voltage and flux vector diagrams are shown in Figure 30. The expressions for the abovementioned conditions are:

$$\begin{aligned} v_s^2 &= v_d^2 + v_q^2 = V_{s\max}^2 \\ i_s^2 &= i_d^2 + i_q^2 = I_{s\max}^2 = I_{qb}^2 \end{aligned} \tag{85}$$

The consequent expressions for reference currents i_d and i_q, derived in Appendix B, are:

$$
\begin{aligned}
i_d &= -I_{qb} K_1 \left(1 - \frac{W_b^2}{w^2} \right) \\
i_q &= I_{qb} \sqrt{1 - \left[K_1 \left(1 - \frac{W_b^2}{w^2} \right) \right]^2}
\end{aligned}
\tag{86}
$$

where
$$K_1 = \frac{I_{qb}}{2I_p} + \frac{I_p}{2I_{qb}} \tag{87}$$

for non-salient PMSM, where $L_d = L_q = L$, and

$$
\begin{aligned}
i_d &= I_p^{'} \left[1 - \sqrt{1 + K_2 \left(1 - \frac{W_b^2}{w^2} \right)} \right] \\
i_q &= I_{qb} \sqrt{1 - \left(\frac{I_p^{'}}{I_{qb}} \right)^2 \left[1 - \sqrt{1 + K_2 \left(1 - \frac{W_b^2}{w^2} \right)} \right]^2}
\end{aligned}
\tag{88}
$$

for a salient machine, where

$$K_2 = \frac{L_{eq}}{L_d} \left(\frac{I_{qb}^2}{I_p^{'2}} \frac{L_q^2}{L_{eq}^2} + 1 \right) \tag{89}$$

$$L_{eq} = \frac{L_q^2 - L_d^2}{L_d} \tag{90}$$

and
$$I_p^{'} = \frac{k_t}{pL_{eq}} \tag{91}$$

Steady-state voltage equations of the salient PMSM when this strategy is applied are:

$$
\begin{aligned}
v_d &\approx -pL_q i_q w = -pL_q I_{qb} \sqrt{w^2 - \left(\frac{I_p^{'}}{I_{qb}} \right)^2 \left[w - \sqrt{w^2 + K_2 \left(w^2 - W_b^2 \right)} \right]^2} \\
v_q &\approx pL_d i_d w + k_t w = pL_d I_p^{'} \left[w - \sqrt{w^2 + K_2 \left(w^2 - W_b^2 \right)} \right] + k_t w
\end{aligned}
\tag{92}
$$

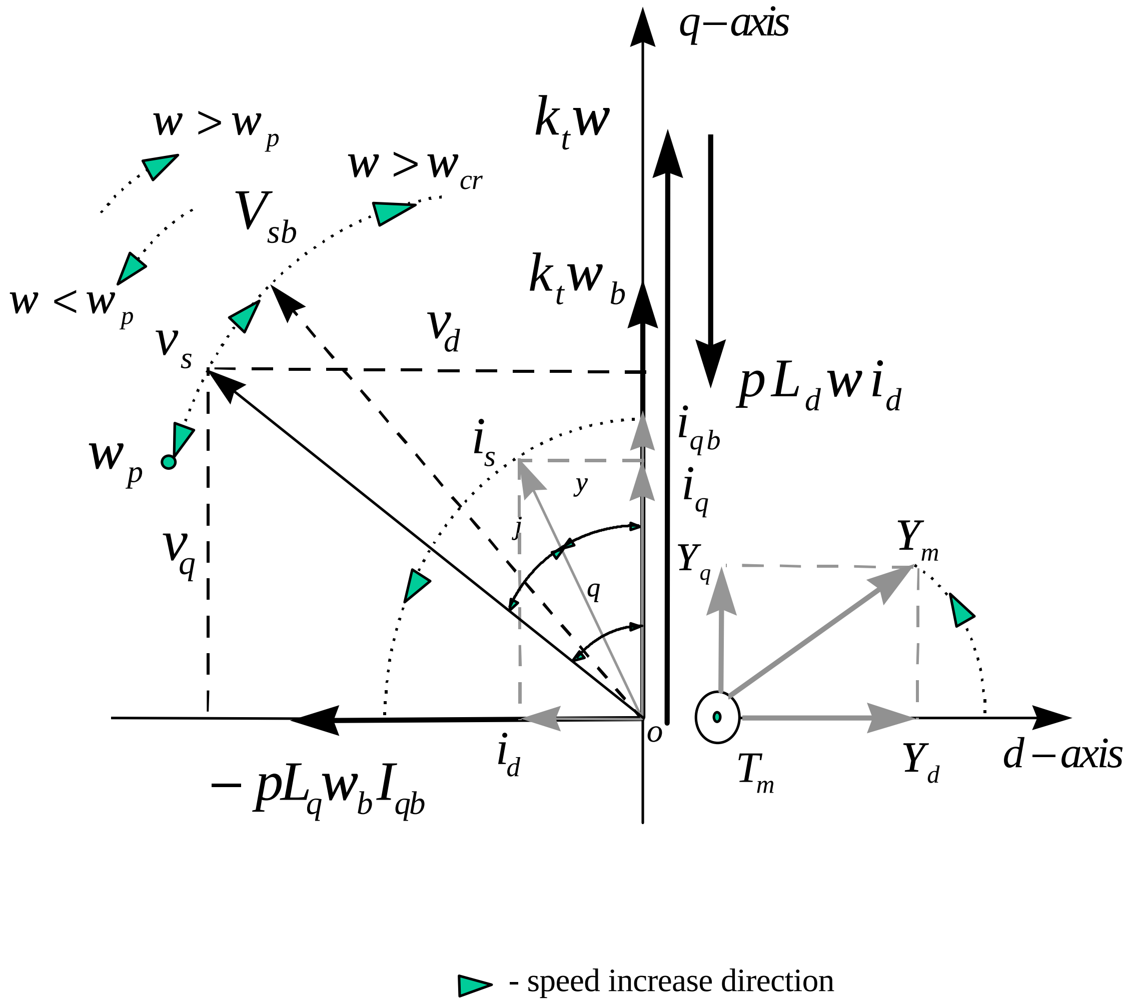

Figure 30. PMSM voltage d-q vector diagram for OCV flux-weakening control

The minimum v_q votage is reached at a prevailing speed ω_p:

$$w_p = W_b \sqrt{\frac{\frac{K_2}{(1+K_2)}}{1-(1+K_2)\left(\frac{L_d^2}{L_q^2}\right)^2}} \Rightarrow v_q = v_{q\,min} \tag{93}$$

All equation derivations are given in Appendix B.

It should be noted from Figure 30 that when $W_b \leq w \leq w_p$, normalized $-i_d$ current (relative to I_{qb}) increase is higher than the normalized speed increase ω_b, which is, on the other side, higher than the normalized i_q current decrease. Consequently, the phase voltage vector v_s rotates toward the negative d-semiaxis. At higher speed these relations are inverse, so that v_s rotates in the opposite direction, i.e. toward the positive q-semiaxis. This observation is useful for the determination of the phase voltage limitation method, discussed earlier in Section 3.2.2.

Although its algorithm is more complicated than those of the constant power flux-weakening control strategies, the advantages regarding the maximum torque profile, maximum exploited power, maximum extended speed for the same amount of energy and keeping constant voltage and constant current amplitudes during the whole period of flux-weakening, without any critical speed point, strongly recommend this strategy against the former ones, whenever the constant active power is not a strong prerequisite. Comparative examples of the discussed methods, applied in a PMSM starter/generator drive are given in Chapter 4.

3.2.3.4 Flux-Weakening Control Small-Signal Models

In order to satisfy assigned power requirements, it can be seen that current references coming from all three mentioned flux-weakening methods must depend on the speed feedback signal. Hence, the additional control loops should be closed and control design becomes much more complex. In order to simplify the analysis of flux-weakening control small-signal models, the following assumptions were made:

1) The speed loop is closed and not saturated; and
2) Small-signal control design is done properly, so that speed follows its reference signal.

These two assumptions allow the flux-weakening input signal to be the speed-reference instead of the speed-feedback signal. In other words, the additional feedback loops are avoided, which preserves the earlier discussed control design procedure. Nevertheless, a brief small-signal analysis of the mentioned flux-weakening techniques still leads to some interesting conclusions regarding the local stability of the flux-weakening control model.

Let’s take a look first at the small-signal derivations (Appendix B) of the constant power control strategies. In order to conserve constant active power through the flux-weakening (speed) region as long as possible, the q-axis reference current, i_q, must follow Eq. (74):

$$i_q = I_{qb} \frac{W_b}{w} \tag{94}$$

Following the small-signal linearization approach, explained in Chapter 2, or simply from i_q current first derivative over speed, its small-signal response to the speed perturbation is:

$$\tilde{i}_q = -I_{qb} \frac{W_b}{W^2} \tilde{w} \tag{95}$$

where Ω is a speed operating point. Such a kind of response is satisfactory, since it is stable in the relative (“per unit”) sense, and it follows the flux-weakening control principle: the higher the speed, the lower the torque, i.e. i_q current. However, the current gain is smaller at higher speed, which makes the control less susceptible to speed change. The analysis of i_d current shows a significant difference between the CVCP and CCCP control strategies. The simplicity of the constant voltage control is the linear relationship between i_d and i_q currents, derived from Eq.s (74) and (76):

$$i_d = -(I_p - \frac{I_p}{I_{qb}} i_q) \tag{96}$$

Consequently, i_d current small-signal response is:

$$\tilde{i}_d = \frac{I_p}{I_{qb}} \tilde{i}_q = -I_p \frac{W_b}{W^2} \tilde{w} \tag{97}$$

The conclusions are the same as for the i_q current.

On the other side, the constant current control implies the non-linear i_d current vs. i_q current relation Eq. (80). That leads to the following i_d current small-signal equation:

$$\tilde{i}_d = \frac{1}{\sqrt{\frac{W^2}{W_b^2} - 1}} \tilde{i}_q = -\frac{I_{qb}}{\sqrt{\frac{W^2}{W_b^2} - 1}} \frac{W_b}{W^2} \tilde{w} \tag{98}$$

Again, the flux-weakening control principle is obeyed: the higher the speed, the higher the (negative) i_d current, the lower the i_q current, i.e. the bigger the flux-weakening. Also, again, the perturbation response is lower at a higher speed. However, it is unstable at $W = W_b$, because of the infinity gain in Eq. (98). In order to get a stable response, some tolerable i_d current must exist before applying this flux-weakening control method. It can be achieved either by entering the flux-weakening region with some other control strategy, like CVCP, until the speed when the gain in Eq. (98) is within tolerable boundaries, or by applying a certain i_d current before the rated speed, i.e. out of the flux-weakening region, like the one for achieving maximum torque control with salient PMSM, calculated from the motor-torque equation in Eq. (12) [70]. Another possibility is to limit the i_d current either to a certain value (it can still result in torque oscillations), or dynamically, with reference to the i_q current, Eq. (80). If none of the above is applied, the high i_d current response at the output of the flux-weakening controller means a high i_d current reference for the current controller, which would saturate the voltage limiters at the controller output, and leave the motor working in an open-loop for a while, what could be intolerable in some applications. The conclusion of this discussion is that, when applying this flux-weakening control strategy, the signal flow should be designed in such a way that the i_q current reference follows from the i_d current reference, nevertheless the i_q current obeys Eq. (94), i.e. the constant power is preserved, at every operating point, or not.

The optimum current vector control small-signal equations, derived from Eq.s (86) and (88) are:

$$\tilde{i}_d = -2I_{qb}K_1\frac{W_b^2}{W^3}\tilde{w} \qquad (99)$$

$$\tilde{i}_q = 2I_{qb}K_1^2\frac{1-\frac{W_b^2}{W^2}}{\sqrt{1-K_1^2\left(1-\frac{W_b^2}{W^2}\right)^2}}\frac{W_b^2}{W^3}\tilde{w} \qquad (100)$$

for a non-salient machine, and

$$\tilde{i}_d = -I_p^{'}K_2\frac{1}{\sqrt{1+K_2\left(1-\frac{W_b^2}{W^2}\right)}}\frac{W_b^2}{W^3}\tilde{w} \qquad (101)$$

$$\tilde{i}_q = \frac{I'_p K_2 \left(1 - \sqrt{1 + K_2 \left(1 - \frac{W_b^2}{W^2} \right)} \right)}{\sqrt{\frac{I_{qb}^2}{I'^2_p} - \left(1 - \sqrt{1 + K_2 \left(1 - \frac{W_b^2}{W^2} \right)} \right)^2} \sqrt{1 + K_2 \left(1 - \frac{W_b^2}{W^2} \right)}} \frac{W_b^2}{W^3} \tilde{w} \tag{102}$$

for a salient machine, respectively.

In both cases, the small-signal response of the i_d current is satisfactory regarding the stability in a relative ("per unit") sense, and it follows the flux-weakening control principle: the higher the speed, the higher the $-i_d$ current. However, the current gain is smaller at higher speed, which, as in constant power strategies, makes the control more difficult.

Regarding the i_q current small-signal response, it has a pole at the speed:

$$W_\infty = \frac{\sqrt{I_p^2 + I_{qb}^2}}{I_p - I_{qb}} W_b \tag{103}$$

for the non-salient machine, and

$$W_\infty = \sqrt{\frac{K_2}{K_2 - \left(\frac{I'_p + I_{qb}}{I'_p} \right)^2 + 1}} W_b \tag{104}$$

for the non-salient machine, where K_2 and I_p' are defined by Eq.s (89) and (91), respectively. The Eq.s (103) and (104) should serve as guidance for the motor drive design when this flux-weakening strategy is chosen, so that speed W_∞ is higher than a desired maximum speed. A deeper analysis of the flux-weakening small-signal relations extends the frame of this work. The purpose of given analysis was to take a designer's attention to several aspects of the small-signal behavior of the discussed flux-weakening control strategies, which has usually been overlooked in flux-weakening control design.